One- and Two-Stage Spatial Amplifiers

Toni Ivanov, *Student Member, IEEE*, Arul Balasubramaniyan, and Amir Mortazawi, *Member, IEEE*

Abstract—**This paper reports the design of nine HEMT, one- and two-stage spatial amplifiers which employ a common ground plane for receiving and transmitting port isolation and for heat sinking. By placing the spatial amplifier array in the near-field of the transmitting and receiving horns, a net gain of 8 dB was obtained. This paper also reports the first demonstration of a two-stage spatial amplifier constructed by employing near-field coupling of two single stage spatial amplifiers in free space.**

I. Introduction

THE INCREASING demand for millimeter-wave communication and radar systems has lead to the need for solid state amplifiers working at these frequencies. However, in order to efficiently amplify electromagnetic waves at these frequencies, conventional amplifier circuits must be modified in order to reduce the losses in the guiding structures. This can be achieved by coupling the waves into and out of the amplifier through free space using radiating elements rather than by conventional waveguide coupling. This approach has lead to increased interest in the area of quasi-optical power amplification [1]–[8]. Quasi-optical amplifiers essentially combine the power of many active devices to exceed the power handling capability of a single solid state device. The first demonstration of a quasi-optical grid amplifier at 3.3 GHz with a gain of 11 dB was reported in [1]. This circuit employs an active grid placed between two orthogonal polarizers which provide the necessary isolation between the input and output ports and serve as tuning elements. Subsequently 16 and 100-element HBT loaded grid amplifiers were reported in [2]. A quasi-optical amplifier based on an integrated horn antenna is described in [3]. This design is uniplanar and compatible with the fabrication process of HEMT transistors. In [4] a quasi-optical power combining transmission amplifier is presented. Antenna arrays, MESFET's, bias and matching circuitry are all contained on a single substrate. A focal point feed that improved the power coupling efficiency was demonstrated in [5]. In [6] folded slot antennas fed by coplanar waveguides were used to improve the bandwidth and to obtain a planar structure. Electromagnetic modeling of these grid array amplifiers can be simplified by electrically isolating unit cells from one another. This approach was demonstrated in [7] where the unit cells were placed in a short section of square waveguide.

In this paper we extend previously reported work [8] and present the results for a narrowband, a broadband, and a two-stage spatial amplifier. These amplifiers were constructed on double layer back-to-back microstrip circuits with a shared ground plane. The continuous ground plane provides a very effective input-output isolation. The ground plane also serves as a heat sink. Furthermore, these circuits can be readily incorporated into multistage spatial amplifiers. In this paper, the results obtained from a two-stage quasi-optical amplifier constructed through near-field coupling of two single stage amplifiers are reported for the first time. The near-field coupling between the stages is advantageous since one can design multistage amplifiers with small interstage spacing (i.e., small fraction of a wavelength). This facilitates the construction of very compact multistage spatial amplifiers.

This paper begins with the discussion of the design methodology and experimental results obtained from fabricating a narrowband spatial amplifier. Subsequently, the results obtained from a broadband spatial amplifier are described. Finally the experimental results from a two-stage amplifier constructed through the coupling of two narrowband spatial amplifiers in series is presented. The coupling between the two stages was accomplished by placing the two stages in the near-field.

II. Single Stage Spatial Amplifiers

A. A Narrowband Spatial Amplifier

To design a multiple device narrowband spatial amplifier, a unit cell is constructed containing only one active device. Fig. 1(a) shows the schematic of a single device amplifier. The active device used is a HEMT (Fujitsu FHX06LG) employed in a common source configuration. In order to design the input and output matching circuits the simultaneous conjugate matched admittances are first determined. Open circuited stubs are used to provide simultaneous conjugate matched susceptances. These stubs effectively resonate the device admittances, hence the admittances seen looking into the input and output ports are purely real. These conductances are then matched to the input and output microstrip antennas using quarter wave transformers. Thus the simultaneous conjugate match conditions are fulfilled.

The circuit layout for a 10 GHz unit cell constructed on a double-layered microstrip structure is shown in Fig. 1(b). To isolate the input and output microstrip antennas, the input and output matching circuits and antennas are fabricated on two separate microstrip circuits which are connected back-to-back with shared ground planes. The two layers are connected through a via hole. The lengths of the microstriplines L_1 and L_2 connected to the input and output terminals of the device are adjusted so that realizable matching circuits can be obtained as described earlier. Suitable stubs and transformers connected at the end of the microstriplines L_1 and L_2 provide

Manuscript received December 31, 1994; revised May 25, 1994. This work was supported in part by Martin Marietta Corporation.

The authors are with the Department of Electrical and Computer Engineering, University of Central Florida, Orlando, FL 32816 USA.

IEEE Log Number 9413425.

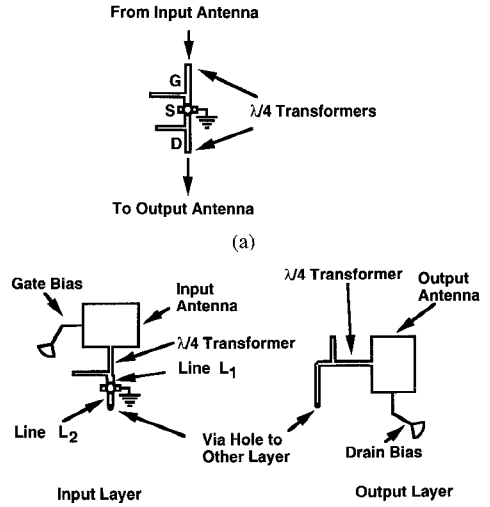

Fig. 1. (a) Schematic of a single device amplifier. (b) Microstrip layout for the unit cell used as a building block for development of a planar array of amplifiers. The single device amplifier [Fig. 1(a)] is fabricated on two different substrates placed back-to-back with shared ground planes.

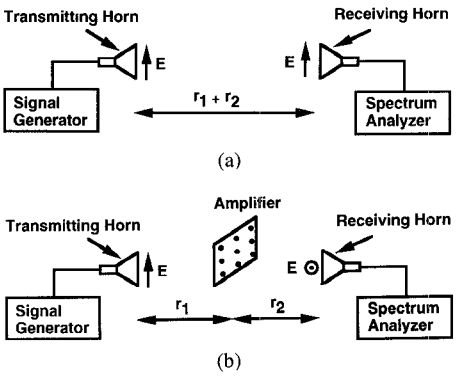

Fig. 2. Measurement setup used to determine the gain of spatial amplifiers. (a) Calibration. The two horn antennas are co-polarized with the amplifier removed from the path of the signal. (b) Gain measurement. The two horn antennas are cross-polarized and the amplifier is placed in the path of the signal.

the required conjugate matched admittances. This matching approach was selected rather than conventional single stub matching since the quarter wave transformers separate the shunt stubs from the radiating edges of the patch antennas. Hence, no additional lines are required to connect the antennas to the matching circuit. The design was done using the CAD tool Libra$^{\text{TM}}$. By incorporating the frequency dependent impedance of the patch antennas into the simulation program, the amplifier's stability was verified. The analysis predicted stability problems from 1 to 2.5 GHz, and in fact the amplifier was stabilized by resistively loading the circuit at low frequencies using a 10 ohm resistor placed along the gate bias lines.

The unit cell was fabricated on 31 mil thick RT Duroid$^{\text{TM}}$ with $\epsilon_r = 2.3$. The active device used is a Fujitsu FHX06FA/LG HEMT biased at $Vds = 2$ V, and $Ids = 10$ mA. The dimensions of the microstrip antennas used are 1.17 cm by 0.91 cm. The microstrip antennas were cross polarized to facilitate the gain measurements. The circuit was biased using high impedance lines connected to the center of the nonradiating edges of microstrip antennas as shown in Fig. 1(b). The setup utilized to measure the spatial amplifier's gain is shown in Fig. 2(a) and (b). The gain of the spatial amplifier can be calculated using the following equation derived from Friis's transmission formula [3]

$$G = \frac{P_r}{P_c} \frac{r_1^2 r_2^2}{(r_1 + r_2)^2} \left(\frac{4\pi}{\lambda}\right)^2 G_{\text{in}}^{-1} G_{\text{out}}^{-1} \tag{1}$$

where r_1 and r_2 are the distances from the circuit to the transmitting and the receiving horn antennas, respectively, and λ is the free space wavelength. G_{in} and G_{out} are the receiving and transmitting microstrip antenna gains as a function of frequency. P_r is the power received by the receiving horn when the two horns are cross polarized with the circuit placed in the path between the two horns [Fig. 2(b)]. P_c is the power received when the two horns are co-polarized with the circuit removed from the path [Fig. 2(a)].

The maximum amplifier gain was measured at 10.4 GHz to be 11.7 dB. The 3 dB bandwidth obtained was 0.25 GHz. In this experiment the calculated directivity of the input and output microstrip antennas as a function of frequency was used to determine the gain and the bandwidth of the spatial amplifier.

An alternate equation [1], developed for grid amplifiers as, was also used as given below

$$G = \frac{P_r}{P_c} \frac{r_1^2 r_2^2}{(r_1 + r_2)^2} \left(\frac{\lambda}{A}\right)^2. \tag{2}$$

Here A is the physical area of the amplifier which can be obtained by multiplying the unit cell area by the number of unit cells used in a multiple device amplifier. P_r, P_c, r_1 and r_2 are similar to the parameters defined in (1). A gain of 10.7 dB was obtained by using this equation. Since the directivity of the antennas used in the spatial amplifiers presented here can readily be calculated, throughout the rest of this paper (1) is used to determine the spatial amplifiers' gain.

First, three unit cells were used to construct a 1×3 spatial amplifier as outlined by the dashed lines in Fig. 3(a) and (b). The inter element spacing was 0.67λ. The bias circuit consisted of high impedance lines connecting the centers of the nonradiating edges of the patch antennas. A maximum measured gain of G =10.4 dB was obtained at 10.04 GHz from this circuit. It should be mentioned that the devices were not selected for uniform characteristics. 10 Ohm resistors were placed along the gate bias lines to stabilize the amplifier at low frequencies.

Next, a 3×3 narrowband spatial amplifier was designed as shown in Fig. 3(a) and (b). The inter element spacing was chosen in order to obtain the maximum directivity from the antenna arrays. This resulted in $0.67 \times 0.75\lambda$ separation between the array elements. The amplifier's gain was measured to be $G = 7.54$ dB at 10.04 GHz with a bandwidth of 0.4 GHz. Fig. 4 shows the gain versus frequency plot for the 3×3 narrowband quasi-optical amplifier. This calculation takes into account the variation of the array gain with frequency. Fig. 5 shows a close match between the theoretical and experimental

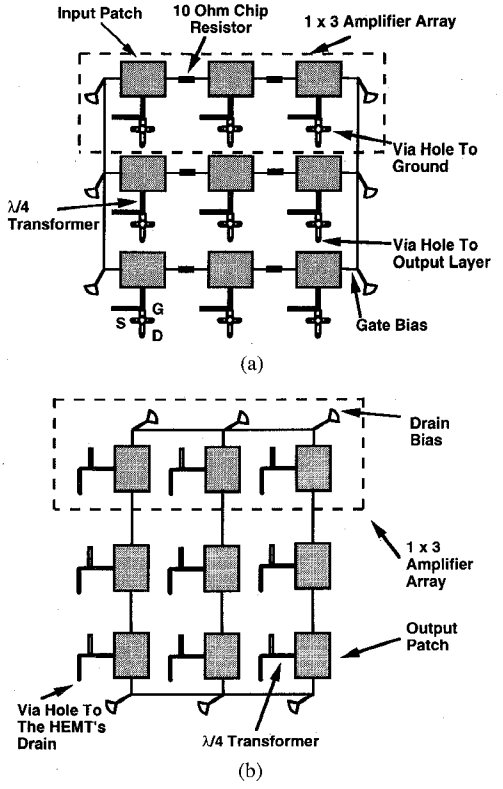

Fig. 3. 3×3 narrowband amplifier layout constructed by replication of the unit cell. (a) Input layer. (b) Output layer.

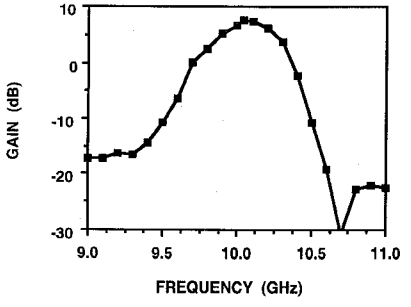

Fig. 4. Gain versus frequency plot for a 3×3 narrowband amplifier.

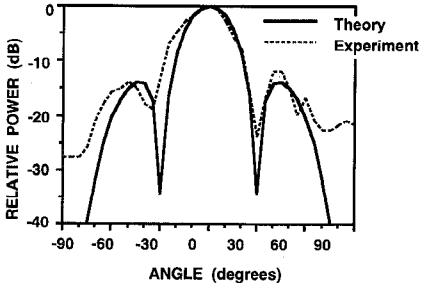

Fig. 5. Theoretical and experimental H-plane patterns for a 3×3 narrowband amplifier.

H-plane patterns. The E-plane pattern was also measured and good agreement with the theoretically predicted pattern was observed.

One can observe that the measured gain of the spatial amplifiers described above dropped as the number of devices in the array increased (i.e., 11.7 dB for the unit cell of the spatial amplifier, 10.3 dB for a 1×3 array and finally 7.54 dB for a 3×3 device amplifier). Several experiments were performed to determine the cause of the gain deterioration. First, the individual active device gains were measured by placing the HEMT's in the single transistor spatial amplifier described previously. The gain of individual devices when biased at the same point (Vds = 2 V, Vgs = − 0.4 V) varied from 7.7 to 11.7 dB. Then, three HEMT's with gains of approximately 8.5 dB were placed in the 1×3 spatial amplifier. The gain of this spatial amplifier was measured to be 8.26 dB. Note that the measured gain for the 1×3 array for randomly selected devices was 10.3 dB. The above measurements indicate that the individual device parameters were different from one another.

This was also observed in the dc operating point of the active devices. The drain current of the individual devices biased at the same Vds and Vgs varied from 6 mA to 15 mA. The results from these experiments confirm that the spatial amplifier gain variations can be attributed to differences in devices characteristics. In monolithic fabrication of such amplifiers this type of problem should not arise since the active devices on a given wafer are expected to have similar characteristics.

B. Near-Field Coupling to Receiving and Transmitting Horns

For some system applications it is important to have a spatial amplifier with net system gain including any actual internal $1/r^2$ losses from the transmitting horn to the plane of the spatial amplifier and from the spatial amplifier to the receiving horn. The set up shown in Fig. 6 was used to eliminate the $1/r^2$ losses internal to the system. This method has advantages over using lenses for focusing since the latter requires finite separation between the receiving and transmitting horns, the focusing lenses, and the spatial amplifier. Thus the overall system size, using the near-field coupling to horns, is reduced. The nine HEMT narrowband amplifier was placed on the aperture of the receiving and transmitting horns. The calibration procedure is shown in Fig. 6(a). The insertion loss of the two horns plus coax to waveguide adapters was 0.3 dB. The power measured at the flange of the receiving horn was used to determine the spatial amplifiers gain. Next, the two horns were cross-polarized and the spatial amplifier was placed between them. The spatial amplifier provided a maximum gain of 8 dB with an input return loss of 6 dB at a frequency of 9.97 GHz. As can be seen the gain of the amplifier is similar to the free space gain measurement mentioned earlier. In order to determine the power combining efficiency of the 9 HEMT spatial amplifier the 1 dB compression point was measured. The output power obtained at the 1 dB compression point was 37.4 mW. Also the 1 dB compression point for a single device amplifier was measured to be 10 mW. Therefore, the power combining efficiency of the 9 HEMT spatial amplifier is 41.5%. The low combining efficiency can mainly be attributed to the nonuniform power distribution across the input horn aperture. This leads to a nonuniform excitation of the amplifier unit cells. In this case the cells close to the center of the

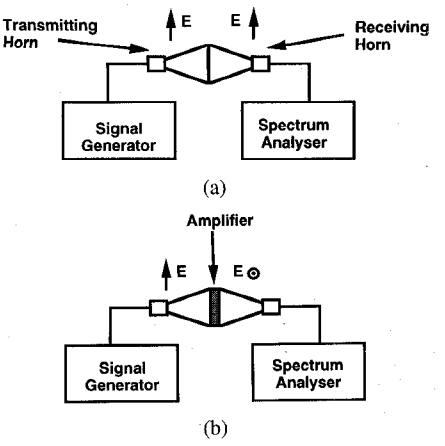

Fig. 6. Measurement setup used to determine amplifier's net gain when it was placed on the aperture of the receiving and transmitting horns. (a) Calibration. The two horn antennas are co-polarized and share a common aperture. (b) Measurement. The two horn antennas are cross-polarized and the amplifier is placed between them.

horn aperture are excited with higher input power than the cells close to the edges. One possible method of exciting the amplifier cells uniformly, is to adjust the width of the patch antennas such that the center devices have patches with smaller widths and to increase the cell density at the center of the horn. Another method is to load the horn antenna with dielectrically filled slots to improve the amplitude uniformity [9], [10].

C. A Broadband Spatial Amplifier

Fig. 7(a) and (b) show the input and output layers of a 3×3 broadband quasi-optical amplifier. The design procedure is similar to the one employed for the narrowband amplifier. In order to increase the bandwidth, the input and output circuits were matched at different frequencies. Libra^{TM} optimization routines were used to obtain maximum gain maintaining the desired bandwidth of 1 GHz. It should be mentioned that the increase in bandwidth was obtained at the expense of the gain. Another difference between the narrowband circuit and the broadband circuit is that, in the latter case, the stubs used to supply the input and output conjugate matched susceptances are connected to each other. Thus they can serve as bias lines for the devices. Such a method of biasing is advantageous since it eliminates the need for the accommodation of extra bias lines.

This circuit was fabricated on a Duroid substrate using the same Fujitsu HEMT devices. The input and output antennas were cross polarized as in the narrowband amplifier. The devices were biased using a single power supply at $V_{DS} = 2.1$ V and total $I_{DS} = 105$ mA. The amplifier's gain was determined using the procedure described previously (Fig. 2). A maximum gain of $G = 6.5$ dB at a frequency of 10.9 GHz with a 3 dB bandwidth of 1 GHz was obtained. Fig. 8 shows the gain versus frequency plot of the broadband amplifier. This calculation takes into account the variation of the array gain with frequency. A plot of the received power as a function of frequency measured by a spectrum analyzer is also shown in the same figure. The two curves have similar shapes. The 1 GHz bandwidth was deduced from the received power curve. Fig. 9 shows the theoretical and experimental E-plane patterns.

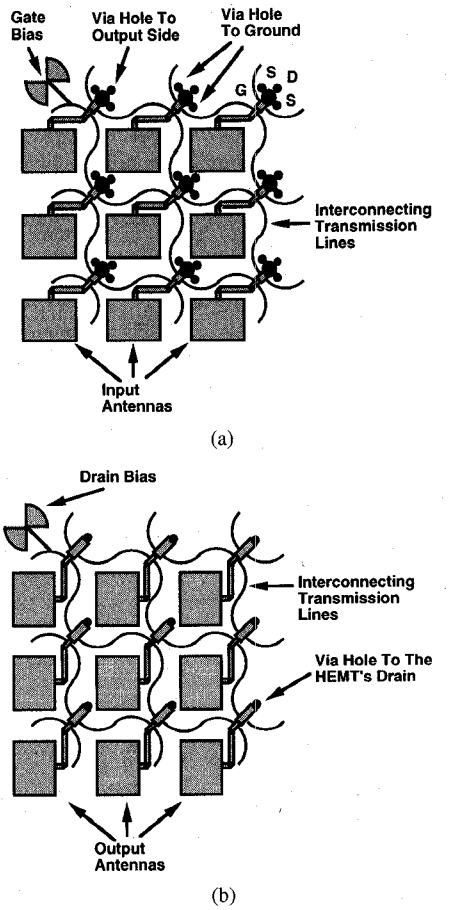

Fig. 7. 3×3 broadband amplifier layout. The circuit is fabricated on two layers, placed back-to-back with shared ground planes. (a) Input layer. (b) Output layer.

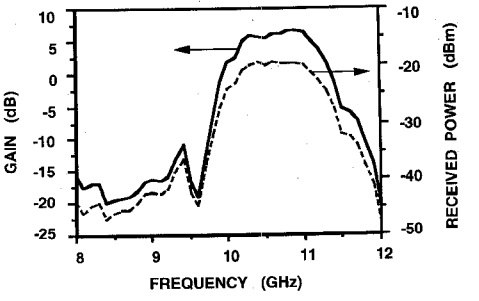

Fig. 8. Gain and actual received power versus frequency plot for a 3×3 broadband amplifier.

III. Two-Stage Quasi-Optical Amplifiers

A. Far-Field Interstage Coupling

In order to achieve higher amplification one can cascade several quasi-optical amplifier layers. In this section the experimental observations made when two quasi-optical stages were placed in the far-field of each other are presented.

A 3×3 narrowband quasi-optical amplifier with a gain of 7.54 dB was discussed previously. A second 3×3 narrowband amplifier array was also fabricated with a gain of 7.34 dB at a frequency of 10.04 GHz under the same bias conditions. These two amplifier stages were placed in the far-fields of each other ($d > 2D^2/\lambda$, where D is the largest linear dimension of the

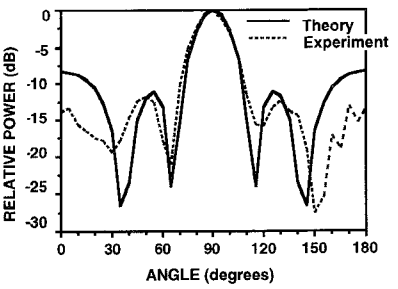

Fig. 9. Theoretical and experimental E-plane patterns for a 3×3 broadband amplifier.

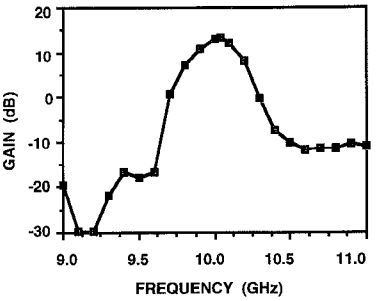

Fig. 11. Gain versus frequency plot for a two-stage 3×3 narrowband amplifier with nearfield separation between the two stages.

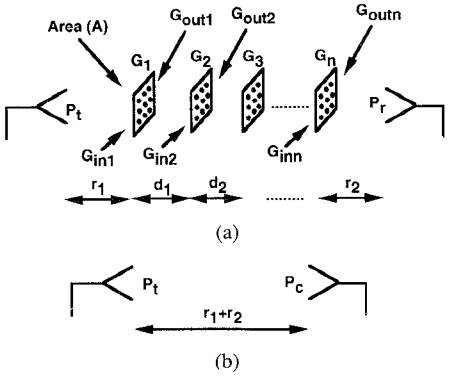

Fig. 10. Multistage spatial amplifier measurement setup. The stages are placed in the farfield of one another. (a) Gain measurement (measurement of Pr). (b) Calibration (measurement of P_c).

circuit) as shown in Fig. 10. In order to determine the gain of a cascaded spatial amplifier (1) and (2) were extended for the general case of n cascaded stages

$$G_1G_2\cdots G_n = \frac{P_r}{P_c}\frac{r_1^2r_2^2}{(r_1+r_2)^2}\left(\frac{4\pi}{\lambda}\right)^2 G_{\text{in1}}^{-1} \cdot G_{\text{out}n}^{-1}\prod_{j=1}^{n-1}\frac{(4\pi d_j)^2}{\lambda^2 G_{\text{out}j}G_{\text{in}(j+1)}} \tag{3}$$

$$G_1G_2\cdots G_n = \frac{P_r}{P_c}\frac{r_1^2r_2^2}{(r_1+r_2)^2}\left(\frac{\lambda}{A_1A_n}\right)^2 \cdot \prod_{j=1}^{n-1}\frac{d_j^2\lambda^2}{A_jA_{j+1}} \tag{4}$$

where $G_1, G_2, \cdots, G_n$ are the gains of the active devices in stage 1, 2, $\cdots, n$, respectively, and $G_{\text{in}j}$ and $G_{\text{out}j}$ are the input and output antenna array gains for the jth stage, respectively. n is the number of stages and the d_ns are the distances of separation between the stages. r_1 and r_2 are the distances from the transmitting horn to the first stage and from the receiving horn to the last stage, respectively. In (4) A_j is the physical area of the jth stage, and d_j is the distance of separation between the j and $j+1$ stages. Equations (3) and (4) give the gain for n cascaded stages, compensating for the power loss due to the spacing between them.

The measured net gains were 13.49 dB and 12.73 dB obtained using (3) and (4), respectively, at 10.04 GHz. These values are close to the sum of the gains of the individual stages. Thus it was verified that both stages deliver gains that are close to the maximum. However, for some system applications the multi stage spatial amplifier should be viewed as a "black box" without correcting for the $1/r^2$ loss due to the separation of individual stages from each other. In this case, the net gain should be calculated using the procedure described in Section I-A for a single stage amplifier by using (1) or (2). The path loss between the different amplifier stages is considered to be inherent to the spatial amplifier and the terms compensating it in (3) and (4) should be neglected. Following this approach the calculated net gain at 10.04 GHz is only 0.34 dB and [0.05 dB using (4)]. One possible way to improve these gains is to use lenses to focus the beam from one stage onto the next stage. Another possible solution is to place the spatial amplifier stages within their near-field regions.

B Near-field Interstage Coupling

In this approach the two amplifier stages were placed within the reactive fields of the corresponding antenna arrays which yields a strong patch to patch coupling. This facilitates the construction of very compact multistage amplifiers (interstage separation of a fraction of a wavelength is possible). Fig. 10 shows the experimental setup of two amplifier stages with near-field interstage separation. The first amplifier stage was positioned at a fixed distance in the far-field of the transmitting horn antenna. The position of the second stage was varied and the stage separation which yielded the maximum gain was determined. It was observed that a maximum gain of $G = 13.34$ [$G = 12.95$ dB using (4)] is obtainable with a separation of $d = 2.5$ cm at a frequency of 10.04 GHz. The gain obtained is quite close to the sum of the gains of the individual stages. Fig. 11 shows the variation of gain versus frequency. The H-plane pattern of the two-stage amplifier with a stage separation of $d = 2.5$ cm was compared with the theoretical H-plane pattern of the 3×3 uniformly excited patch array in Fig. 12. As can be observed, the main lobe of the H-plane pattern has not changed significantly.

The gain obtained for the two-stage amplifier was determined as a function of interstage separation. Fig. 13 shows the variation of net gain versus distance of separation d. Successive maxima of gain were observed with a periodicity $d = \lambda_o/2$.

This experiment clearly demonstrates the advantages of near-field coupling between the stages of the multistage cascaded spatial amplifiers presented in this paper.

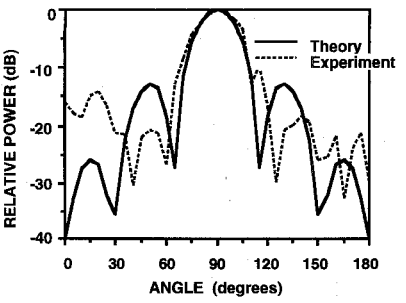

Fig. 12. Comparison of measured H-plane pattern for a two stage 3×3 amplifier utilizing nearfield coupling between the two stages with theoretical H-plane pattern of a 3×3 patch array.

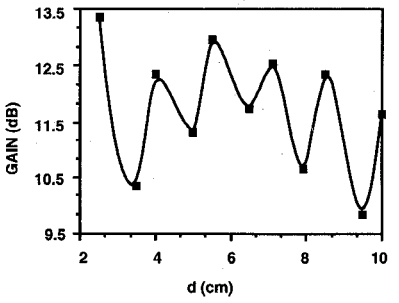

Fig. 13. Net gain versus distance of separation "*d*" for a two-stage amplifier utilizing nearfield coupling.

IV. Conclusion

Narrowband and broadband quasi-optical amplifiers on double layer microstrip circuits have been demonstrated. The common ground plane between the input and output ports provides effective signal isolation and device heat sinking. Also the near-field coupling of the transmitting and receiving horns to the spatial amplifier was demonstrated. The results obtained from a two-stage spatial amplifier by employing the near-field coupling of two single stage amplifiers were also reported. This paper demonstrated the feasibility of obtaining net gain through the near-field coupling of spatial amplifiers. A detailed study of the near-field coupling between the stages is underway.

Acknowledgment

The authors would like to thank Fujitsu Corp. for donating the HEMT's and Rogers Corp. for donating the substrate material.

References

[1] M. Kim, J. Rosenberg, R. P. Smith, R. M. Weikle, J. B. Hacker, M. P. Delisio, and D. B. Rutledge, "A grid amplifier," *IEEE Microwave and Guided Wave Lett.*, vol. 1, no. 11, pp. 322–324, Nov. 1991.

[2] M. Kim, E. A. Sovero, J. B. Hacher, M. P. DeLisio, J. C. Chiao, S. J. Li, D. R. Cagnon, J. J. Rosenberg, and D. B. Rutledge, "A 100-element HBT grid amplifier," in *IEEE MTT-S Int. Microwave Symp. Dig.*, June 1993, pp. 615–618.

[3] C. Y. Chi and G. M. Rebeiz, "A quasi-optical amplifier," *IEEE Microwave and Guided Wave Lett.*, vol. 3, no. 6, pp. 164–166, June 1993.

[4] T. Mader, J. Schoenberg, L. Harmon, and Z. B. Popovic, "Planar MESFET transmission wave amplifier," *Electron. Lett.*, vol. 29, no. 19, pp. 1699–1701, Sept. 1993.

[5] J. S. H. Schoenberg and Z. B. Popovich, "Planar lens amplifier," in *IEEE Microwave Theory Tech.-S Int. Microwave Symp. Dig.*, May 1994, pp. 429–432.

[6] H. S. Tsai and R. A. York, "Polarization-rotating quasi-optical reflection amplifier cell," *Electron. Lett.*, vol. 29, pp. 2125–2127, Nov. 1993.

[7] N. J. Kolias and R. C. Compton, "A microstrip-based unit cell for quasi-optical amplifier arrays," *IEEE Microwave and Guided Wave Lett.*, vol. 3, no. 9, pp. 330–332, Sept. 1993.

[8] N. Sheth, T. Ivanov, A. Balasubramanniyan, and A. Mortazawi, "A nine HEMT spatial amplifier," in *IEEE Microwave Theory Tech.-S Int. Microwave Symp. Dig.*, May 1994, pp. 1239–1242.

[9] J. A. Benet, A. R. Perkons, S. H. Wong, and A. Zaman, "Spatial power combining for millimeterwave solid state amplifiers," in *IEEE Microwave Theory Tech.-S Int. Microwave Symp. Dig.*, June 1993, pp. 619–622.

[10] M. S. Aly and S. F. Mahmud, "Propagation and radiation behavior of a longitudinally slotted horn with dielectrically filled slots," *IEE Proc.*, vol. 132, no. 7, pp. 477–479, Dec. 1985.

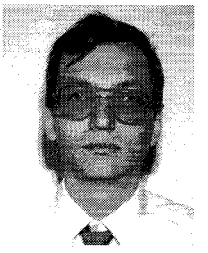

Toni Ivanov (S'93) was born in Varna, Bulgaria, in 1962. He received the B.S. degree in electrical engineering from Higher Institute of Mechanics, St. Petersburg, Russia, in 1989, and the M.S.E.E. degree from University of Central Florida, Orlando, FL, in 1994.

He is currently with the Department of Electrical and Computer Engineering, at the University of Central Florida, working toward the Ph.D. degree. His research interests include quasi-optical power combining techniques, oscillator and amplifier design for high power MMIC applications and printed mm-wave antennas.

Arul Balasubramaniyan was born in Madras, India, in 1971. He received the B.S. degree in electrical engineering from Anna University, India, in 1991, and the M.S.E.E. degree from University of Central Florida, Orlando, FL, in 1994.

He is currently an RF Engineer with Motorola, Fortworth, TX. His technical interests include analog IC design, MMIC design and communication theory.

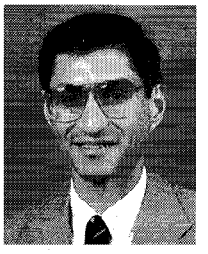

Amir Mortazawi (S'87–M'90) was born in Iran in 1962. He received the B.S. degree in electrical engineering from the State University of New York at Stony Brook in 1987 and the M.S. and Ph.D. degrees in electrical engineering from the University of Texas at Austin, in 1988 and 1990, respectively.

In 1990, he joined the University of Central Florida, where he is currently an Associate Professor. His research interests include millimeter-wave power combining oscillators and amplifiers, quasi-optical techniques and nonlinear analysis of microwave circuits.

Dr. Mortazawi is a member of Tau Beta Pi and Eta Kappa Nu.